

Stagnation-point Flow and Mass Transfer with Chemical Reaction Past a Permeable Stretching/Shrinking Sheet in a Nanofluid

(Aliran Titik Genangan dan Pemindahan Jisim dengan Tindak Balas Kimia Terhadap Helaian Meregang/Mengecut Telap dalam Nanobendalir)

NATALIA C. ROSCA, TEODOR GROSAN & IOAN POP*

ABSTRACT

*A numerical study has been conducted to investigate the steady forced convection stagnation point-flow and mass transfer past a permeable stretching/shrinking sheet placed in a copper (Cu)- water based nanofluid. The system of partial differential equations is transformed, using appropriate transformations, into two ordinary differential equations, which are solved numerically using *bvp4c* function from Matlab. The results are obtained for the reduced skin-friction and reduced Sherwood number as well as for the velocity and concentration profiles for some values of the governing parameters. These results indicate that dual solutions exist for the shrinking sheet case ($\lambda < 0$). It is shown that for a regular fluid ($\phi = 0$) a very good agreement exists between the present numerical results and those reported in the open literature.*

Keywords: Mass transfer; nanofluid; permeable sheet; stretching/shrinking sheet

ABSTRAK

*Suatu kajian berangka telah dijalankan bagi mengkaji aliran titik genangan olakan paksa mantap dan pemindahan jisim terhadap helaian meregang/mengecut telap di dalam nanobendalir berasaskan air-kuprum (Cu). Sistem persamaan pembezaan separa dijelmakan kepada dua persamaan pembezaan biasa dengan penjelmaan yang bersesuaian, yang diselesaikan secara berangka menggunakan fungsi *bvp4c* daripada perisian Matlab. Keputusan diperoleh bagi geseran kulit terturun dan nombor Sherwood terturun, serta profil halaju dan kepekatan bagi beberapa nilai parameter menakluk. Keputusan menunjukkan yang penyelesaian dual wujud bagi kes helaian mengecut ($\lambda < 0$). Didapati bahawa bagi bendalir biasa atau asas ($\phi = 0$), hasil perbandingan yang sangat baik diperoleh antara keputusan berangka terkini dengan keputusan yang dilaporkan oleh penyelidik terdahulu.*

Kata kunci: Helaian meregang/mengecut; helaian telap; nanobendalir; pemindahan jisim

INTRODUCTION

The study of forced convection flow over a stretching (or shrinking) sheet has many applications in industries. For example, the thermal processing of sheet-like materials occurs in the production of paper, linoleum, polymeric sheets, roofing shingles, insulating materials, fine-fiber mattes and boundary layer along a liquid film in condensation processes (Sparrow & Abraham 2005). The moving sheet induces motion in the neighboring fluid or, alternatively, the fluid may have an independent forced-convection motion that is parallel to that of the sheet. It is very important to control the drag and the heat flux for better product quality. The study of laminar flow over stretching sheets is currently attracting the attention of a growing number of researchers because of the immense potential of nanofluids. Such applications can be found in food processing, transpiration cooling, reactor fluidization. The rate of heat and mass transfer within the boundary layer has a direct bearing on the success of the coating process and the chemical characteristics of the product.

Crane (1970) presented an exact solution of the two-dimensional Navier-Stokes equations for a stretching sheet problem. Gupta (1977) considered the effect of mass transfer on the Crane flow. Miklavčič and Wang (2006) investigated the flow over a shrinking sheet, which is an exact solution of the Navier-Stokes equations and it was shown that in order to maintain the flow over the shrinking sheet mass suction is required. Fang et al. (2008, 2009) and Fang (2008) investigated the flow induced by a shrinking sheet. The two-dimensional stagnation-point flow past a shrinking sheet was studied by Wang (2008). Goldstein (1965) has shown that this flow is essentially a backward flow and it shows different physical phenomena than the stretching flow.

In order to improve heat and mass transfer in viscous fluids, a small fraction of solid nanoparticles has to be added. The term nanofluid has been suggested by Choi (1995) and it refers to fluids in which nano-scale particles are suspended in the base fluid. The behavior of nanofluids provides a basis for heat transfer intensification in industrial

sectors including transportation, power generation, thermal therapy for cancer treatment, chemical sectors, ventilation, air-conditioning, etc (Ding et al. 2007). References on nanofluids can be found in the book by Das et al. (2007) and in the review papers by Buongiorno (2006), Eagen et al. (2010), Fan and Wang (2011), Kakaç and Pramuanjaroenkij (2009), Lee et al. (2010), Wang and Mujumdar (2008) and Wong & Leon (2010). It is worth mentioning to this end, that stretching problems in nanofluids were studied by Bachok et al. (2010a, 2010b), Khan & Pop (2010) and Yacob et al. (2011).

The aim of this paper was to investigate the steady forced convection stagnation point-flow and mass transfer past a permeable stretching/shrinking sheet placed in a nanofluid using the mathematical nanofluid model proposed by Tiwari and Das (2007). Employing appropriate similar variables the partial differential equations were transformed into ordinary differential equations, which have been solved numerically. The effects of the pertinent parameters such as solid nanofluid volume fraction, stretching/shrinking, mass transfer and chemical reaction rate on the flow and mass flux characteristics have been studied.

BASIC EQUATIONS

Consider the steady two-dimensional boundary layer flow of a nanofluid near the stagnation point on a permeable linearly stretching/shrinking sheet with chemically reactive species undergoing first order chemical reaction. It is assumed that the velocity of the stretching/shrinking sheet is $u_w(x) = cx$ and that of the external (inviscid) flow is $u_e(x) = ax$, where a and c are constants with $a > 0$ and $c > 0$ for a stretching sheet and $c < 0$ for a shrinking sheet, respectively. It is also assumed that the constant concentrations at the surface of the sheet and in the external flow are C_w and C_∞ , respectively. The physical model and the coordinate system is shown in Figure 1, where x and y are coordinates measured along the surface of the sheet and normal to it, respectively. Under these assumptions, the boundary layer equations of continuity, motion and solute distribution can be written as:

$$\frac{\partial u}{\partial x} + \frac{\partial v}{\partial y} = 0, \tag{1}$$

$$u \frac{\partial u}{\partial x} + v \frac{\partial u}{\partial y} = u_e \frac{du_e}{dx} + \frac{\mu_{nf}}{\rho_{nf}} \frac{\partial^2 u}{\partial y^2}, \tag{2}$$

$$u \frac{\partial C}{\partial x} + v \frac{\partial C}{\partial y} = D \frac{\partial^2 C}{\partial y^2} - R(C - C_\infty), \tag{3}$$

subject to the boundary conditions

$$\begin{aligned} u &= u_w(x) = cx, v = v_0, C = C_w \text{ at } y = 0 \\ u &\rightarrow u_e(x) = ax, C \rightarrow C_\infty \text{ as } y \rightarrow \infty. \end{aligned} \tag{4}$$

Here u and v are the velocity components along x and y directions, v_0 is the mass flux velocity with $v_0 < 0$ for suction and $v_0 > 0$ for injection (or blowing), respectively, C is the mass concentration of the nanofluid, D is the diffusion coefficient and R denotes the reaction rate of the solute. Further, μ_{nf} is the dynamic viscosity of the nanofluid and ρ_{nf} is the density of the nanofluid, which are given in Table 1 (Oztop & Abu-Nada 2008)

$$\mu_{nf} = \frac{\mu_f}{(1-\phi)^{2.5}}, \rho_{nf} = (1-\phi)\rho_f + \phi\rho_s, \tag{5}$$

where ϕ is the nanoparticle volume fraction, μ_f is the dynamic viscosity of the base fluid, ρ_f is the density of the base fluid and ρ_s is the density of the solid particle. The dynamic viscosity of the nanofluid μ_{nf} has been proposed by Brinkman (1952). It is worth mentioning that the expressions (5) are restricted to spherical nanoparticles, where it does not account for other shapes of nanoparticles.

We introduce now the stream function ψ defined as $u = \partial\psi/\partial y$ and $v = -\partial\psi/\partial x$. Equations (2) and (3) become:

$$\frac{\partial \psi}{\partial y} \frac{\partial^2 \psi}{\partial x \partial y} - \frac{\partial \psi}{\partial x} \frac{\partial^2 \psi}{\partial y^2} = u_e \frac{du_e}{dx} + \frac{\mu_{nf}}{\rho_{nf}} \frac{\partial^3 \psi}{\partial y^3}. \tag{6}$$

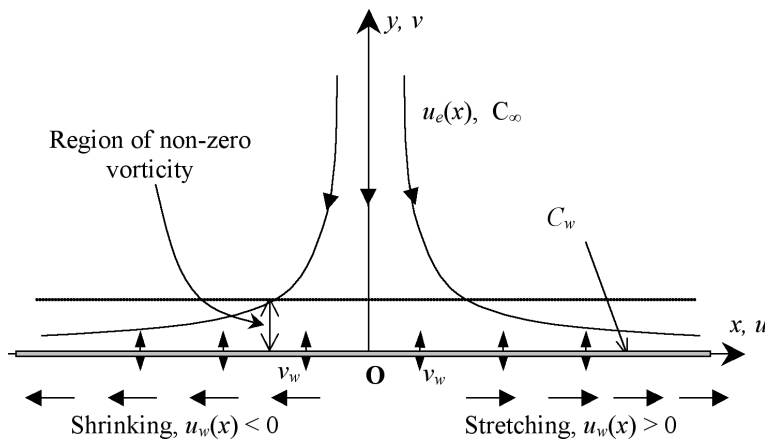


FIGURE 1. Physical model and coordinate system

TABLE 1. Physical properties of fluid and nanoparticles

Property	Water	Cu	Al ₂ O ₃	TiO ₂
c_p (J/kg K)	4179	385	765	686.2
ρ (kg/m ³)	997.1	8933	3970	4250
k (W/m K)	0.613	400	40	8.9538
$\alpha \times 10^7$ (m ² /s)	1.47	1163.1	131.7	30.7
$\beta \times 10^{-5}$ (1/K)	21	1.67	0.85	0.9

$$\frac{\partial \psi}{\partial y} \frac{\partial C}{\partial x} - \frac{\partial \psi}{\partial x} \frac{\partial C}{\partial y} = D \frac{\partial^2 C}{\partial y^2} - R(C - C_\infty), \quad (7)$$

and the boundary conditions (4) become:

$$\begin{aligned} \frac{\partial \psi}{\partial y} &= cx, \quad \frac{\partial \psi}{\partial x} = -v_0, \quad C = C_w \quad \text{at } y = 0 \\ \frac{\partial \psi}{\partial y} &\rightarrow ax, \quad C \rightarrow C_\infty \quad \text{as } y \rightarrow \infty. \end{aligned} \quad (8)$$

Next, we look for a similarity solution of Equations (6) and (7) of the following form:

$$\psi = (av_f)^{1/2} xf(\eta), \quad C = C_\infty + (C_w - C_\infty) \theta(\eta), \quad \eta = (a/v_f)^{1/2} y \quad (9)$$

where v_f is the kinematic viscosity of the base fluid. Thus, the partial differential equations (6) and (7) are transformed into the following ordinary (similarity) differential equations:

$$\frac{1}{(1-\phi)^{2.5} (1-\phi + \phi \rho_s / \rho_f)} f''' + ff'' - f'^2 + 1 = 0 \quad (10)$$

$$\theta'' + Sc f \theta' - Sc \beta \theta = 0, \quad (11)$$

where $Sc = v_f / D$ is the Schmidt number and $\beta = R/a$ is the reaction-rate parameter. The boundary conditions (8) become:

$$\begin{aligned} f(0) &= s, \quad f'(0) = \lambda, \quad \theta(0) = 1 \quad \text{at } \eta = 0 \\ f'(\eta) &\rightarrow 1, \quad \theta(\eta) \rightarrow 0 \quad \text{as } \eta \rightarrow \infty, \end{aligned} \quad (12)$$

where $s = -v_0 / (av_f)^{1/2}$ is the mass transfer parameter with $s > 0$ for suction and $s < 0$ for injection, respectively, and $\lambda = c/a$ is the stretching parameter with $\lambda > 0$ for stretching and $\lambda < 0$ for shrinking sheet, respectively. It is worth mentioning to this end that when $\phi = 0$ (regular fluid) and $s = 0$ (impermeable sheet), Equation (10) and (11) reduce to those found by Bhattacharyya (2011).

The quantities of physical interest are the skin friction coefficient C_f and the local Sherwood number Sh_x , which are defined as:

$$C_f = \frac{\tau_w}{\rho_f u_e^2}, \quad Sh_x = \frac{x q_m}{D(C_w - C_\infty)}, \quad (13)$$

where τ_w is the wall shear stress and q_m is the wall mass concentration flux, which are defined as:

$$\tau_w = \mu_{nf} \left(\frac{\partial u}{\partial y} \right)_{y=0}, \quad q_m = -D \left(\frac{\partial C}{\partial y} \right)_{y=0}. \quad (14)$$

Using variables (9), we obtain:

$$\text{Re}_x^{1/2} C_f = \left(\frac{\mu_{nf}}{\mu_f} \right) f''(0), \quad \text{Re}_x^{-1/2} Sh_x = -\theta'(0). \quad (15)$$

NUMERICAL RESULTS AND DISCUSSION

The considered problem is formulated in such a way so that we can consider different types of nanoparticles (Cu, Al₂O₃, TiO₂, etc.) and water as a base fluid. However, in order to save space, we will consider here only the case of Cu nanoparticles. The ordinary differential equations (ODEs) (10) and (11) subject to the boundary conditions (12), were solved numerically using the function `bvp4c` from Matlab. To accomplish this, the first step is to write Equations (10) and (11) as a system of first order differential equations by introducing new variables, one for each variable in the original problem plus one for each derivative up to the highest order derivative minus one. The `bvp4c` function implements a collocation method for the solution of the following boundary value problem

$$y' = f(x, y), \quad a \leq x \leq b, \quad (16)$$

subject to the two-point boundary conditions:

$$bc(y(a), y(b)) = 0. \quad (17)$$

The approximate solution $S(x)$ is a continuous function that is a cubic polynomial on each subinterval $[x_n, x_{n+1}]$ of the mesh $a = x_0 < x_1 < \dots < x_N = b$. It satisfies the boundary conditions:

$$bc(S(a), S(b)) = 0, \tag{18}$$

and it also satisfies the following differential equations (collocates) at both ends and mid-point of each subinterval:

$$S'(x_n) = f(x_n, S(x_n)). \tag{19}$$

$$S'((x_n + x_{n+1})/2) = f((x_n + x_{n+1})/2, S((x_n + x_{n+1})/2)). \tag{20}$$

$$S'(x_{n+1}) = f(x_{n+1}, S(x_{n+1})). \tag{21}$$

These conditions result in a system of nonlinear algebraic equations for the coefficients defining $S(x)$, which are solved iteratively by linearization. Here $S(x)$ is a fourth order approximation to an isolated solution $y(x)$, i.e., $\|y(x) - S(x)\| \leq Ch^4$, where h is the maximum of the step sizes $h_n = x_{n+1} - x_n$ and C is a constant. For such an approximation, the residual $r(x)$ in the ODEs is defined by:

$$r(x) = S'(x) - f(x, S(x)). \tag{22}$$

Mesh selection and error control are based on the residual of the continuous solution. The relative error tolerance was set to 10^{-10} . In this method, we have chosen a suitable finite value of $\eta \rightarrow \infty$, namely $\eta = \eta_\infty = 10$.

Since the present problem may have more than one (dual) solution, the `bvp4c` function requires an initial guess of the desired solution for the ODEs (10) and (11). The guess should satisfy the boundary conditions and reveal the behavior of the solution. Determining an initial guess for the first (upper branch) solution is not difficult because the `bvp4c` method will converge to the first solution even for poor guesses. However, it is difficult to come up with a sufficiently good guess for the second (lower branch)

solution of the system of ODEs (10) and (11). To overcome this difficulty, we start with a set of parameter values for which the problem is easy to be solved. Then, we use the obtained result as initial guess for the solution of the problem with small variation of the parameters. This is repeated until we reach the right values of the parameters. This technique is called continuation (Shampine et al. 2010).

The numerical computations are performed for several values of the dimensionless parameters involved in the equations, such as the stretching/shrinking parameter λ , suction/injection parameter s , nanofluid volume fraction parameter ϕ , Schmidt number Sc and the reaction-rate parameter β . As in Oztop & Abu-Nada (2008), we take the values of the solid volume fraction ϕ in the range $0 \leq \phi \leq 0.2$. To validate the accuracy of the numerical scheme, a comparison of the obtained results corresponding to the reduced skin friction coefficient $f''(0)$ is made with the available published results of Bhattacharyya (2011) and Ishak et al. (2010) for several values of λ when $\phi = 0$ (regular fluid) and $s = 0$ (impermeable sheet). This comparison is shown in Table 2 and it is found that the results are in excellent agreement. It, therefore, gives us the confidence that the present results are accurate.

Figures 2 to 6 show the variation of the reduced skin friction coefficient $f''(0)$ and the concentration gradient at the sheet $-\theta'(0)$ (which is proportional to the rate of mass transfer from the sheet) with λ for several values of $s = 0, 1, 2$ and $\phi = 0, 0.1, 0.2$ when the Schmidt number Sc and reaction-rate parameter β take the values $Sc = \beta = 1$. It is evident from these figures that multiple (dual) solutions of Equation (10) and (11) subject to the boundary conditions (12) exist (upper and lower branch solutions) when $\lambda < 0$ (shrinking sheet). Which solution actually occurs depend on the flow stability, which is not investigated in this paper. There exists a critical value $\lambda_c < 0$ of $\lambda < 0$ for which the upper branch solution meets the lower branch solution, respectively. It is seen from Figure 2 that in the case when $s = 0$ the solutions for $f''(0)$ are unique when $\lambda > -1$, dual when $\lambda_c \leq \lambda \leq -1$ and no solution when $\lambda < \lambda_c < 0$. Further, in the case $s = 2$ the solutions for $f''(0)$ are unique when λ

TABLE 2. Comparison of the values of $f''(0)$ for several values of λ when $\phi = 0$ and $s = 0$

λ	Present study		Bhattacharyya (2011)		Ishak et al. (2010)	
	First solution	Second solution	First solution	Second solution	First solution	Second solution
-0.25	1.4022407		1.4022405		1.402241	
-0.50	1.4956697		1.4956697		1.495670	
-0.75	1.4892981		1.4892981		1.489298	
-1.00	1.3288168	0	1.3288169	0	1.328817	0
-1.15	1.0822311	0.1167020	1.0822316	0.1167023	1.082231	0.116702
-1.20	0.9324733	0.2336496	0.9324728	0.2336491	0.932474	0.233650
-1.2465	0.5842816	0.5542962	0.5842915	0.5542856	0.584295	0.554283
-1.24657	0.5745372	0.5640096	0.5745268	0.5639987		

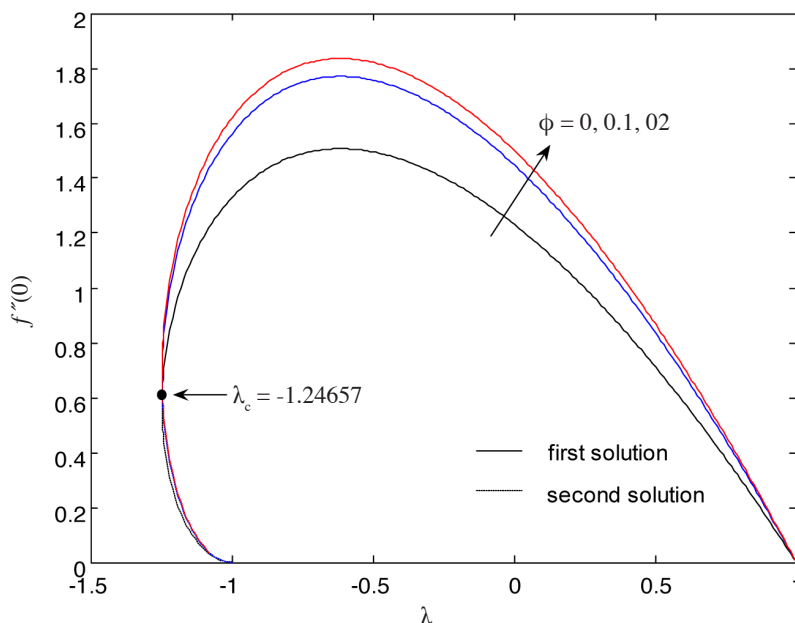


FIGURE 2. Variation of $f''(0)$ with λ for $\phi = 0, 0.1, 0.2$ when $s = 0$

> -0.4 , dual when $\lambda_c \leq \lambda \leq -0.4$ and no solution when $\lambda < \lambda_c < 0$ (Figure 3), while in the case when $\phi = 0.1$ the solutions for $f''(0)$ are unique when $\lambda > -1$, dual when $\lambda_c \leq \lambda \leq -1$ and no solution when $\lambda < \lambda_c < 0$ (Figure 4). Beyond λ_c the boundary layer separates from the surface of the sheet, thus no solution is obtained. Based on our computation, $\lambda_c = -1.24657$ when $s = 0$ and $\phi = 0, 0.1, 0.2$ (Figure 2). For $s = 2$, $\lambda_c = -2.9270$ when $\phi = 0$, $\lambda_c = -3.3850$ when $\phi = 0.1$ and $\lambda_c = -3.5065$ when $\phi = 0.2$ (Figure 3). For $\phi = 0.1$, $\lambda_c = -1.24657$ when $s = 0$, $\lambda_c = -2.0446$ when $s = 1$ and $\lambda_c = -3.3850$ when $s = 2$ (Figure 4). These results show that $|\lambda_c|$ increases with increasing

ϕ . It can be also seen that the value of $|\lambda_c|$ is greater for nanofluid ($\phi \neq 0$) than for a regular fluid ($\phi = 0$). On the other hand, Figures 5 and 6 display the variation of the concentration gradient at the sheet $-\theta'(0)$ with λ for $\phi = 0, 0.1, 0.2$ when $s = 2$, $Sc = 1$ and $\beta = 1$ (Figure 5) and the variation of $-\theta'(0)$ with λ for $s = 0, 1, 2$ when $\phi = 0.1$, $Sc = 1$ and $\beta = 1$ (Figure 6). In these cases, λ_c takes the same values as for $f''(0)$. Also $-\theta'(0)$ increases with ϕ indicating a better concentration gradient at the sheet. Thus, the parameters ϕ , λ and s can be used to control the magnitude of the skin friction coefficient and the local Sherwood number.

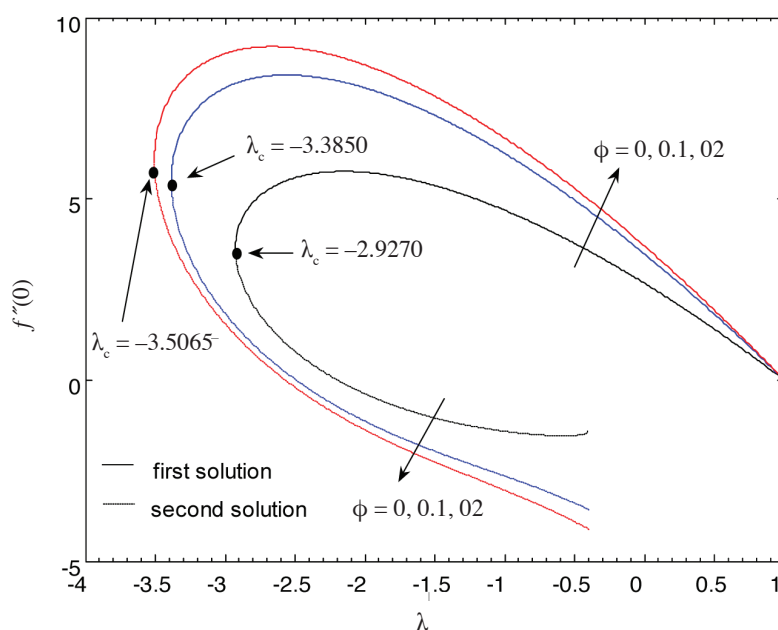


FIGURE 3. Variation of $f''(0)$ with λ for $\phi = 0, 0.1, 0.2$ when $s = 2$

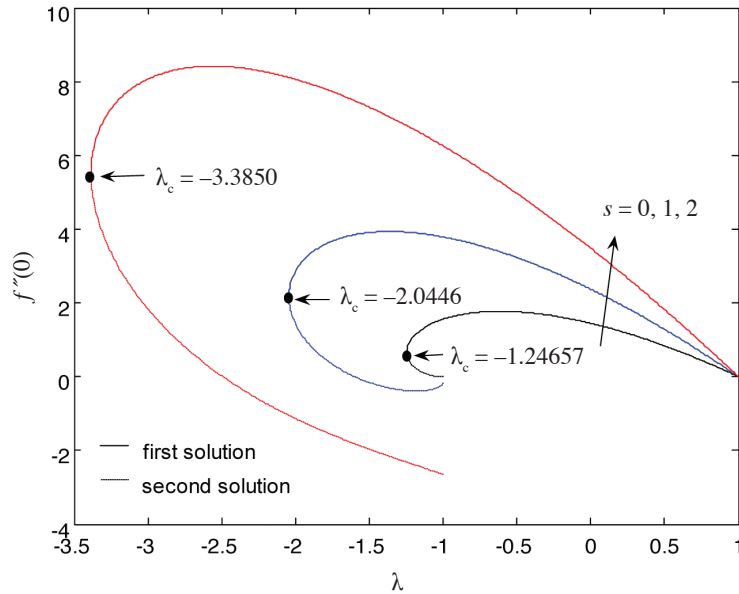


FIGURE 4. Variation of $f''(0)$ with λ for $s = 0, 1, 2$ when $\phi = 0.1$

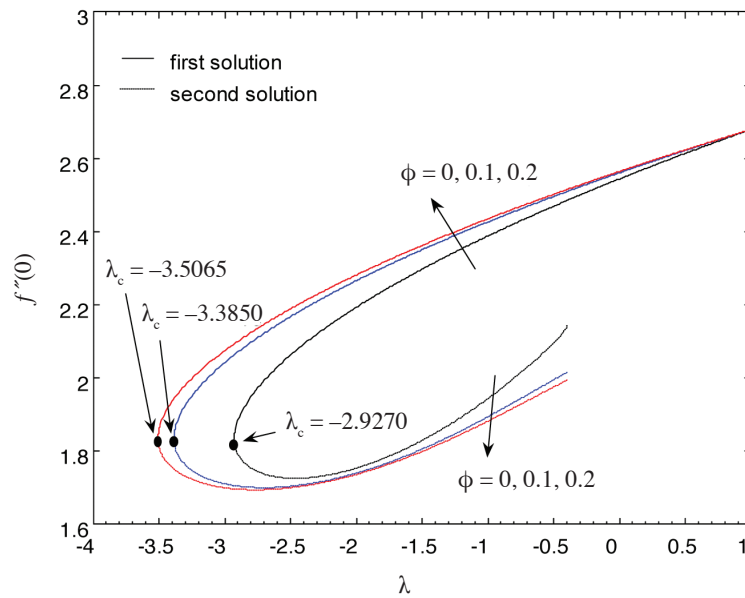


FIGURE 5. Variation of $-\theta'(0)$ with λ for $\phi = 0, 0.1, 0.2$ when $s = 2, Sc = 1$ and $\beta = 1$

The velocity $f'(\eta)$ and concentration $\theta(\eta)$ profiles are presented for different values of the parameters considered in Figures 7 and 8. It is observed that the lower branch profiles also satisfy the far field boundary conditions asymptotically, thus support the validity of the present results. Besides supporting the dual nature of the solution to the boundary value problem (10) and (11) presented in Figures 2 to 6, both Figure 7 and 8 show that the boundary layer thickness is higher for the second (lower branch) solution compared to the first (upper branch) solution, which in turn produces higher values of $f''(0)$ and $-\theta'(0)$. Finally, values of the reduced skin friction $f''(0)$ and Sherwood number $-\theta'(0)$ for $\lambda = 0, 0.1, 1, 10$ when $s = 0,$

$1, 2, \phi = 0, 0.1, 0.2, Sc = 1$ and $\beta = 1$ are given in Table 3. It is to be noticed that for $\lambda < 1$ and a fixed value of s , both $f''(0)$ and $-\theta'(0)$ increase with ϕ , while $f''(0)$ and $-\theta'(0)$ decrease with ϕ when λ is large and s is fixed.

CONCLUSION

We extended the classical problem of the steady stagnation-point flow and mass transfer with the first order chemical reaction by considering a permeable stretching/shrinking sheet in a nanofluid. The transformed ODEs are solved numerically by using the function `bvp4c` from Matlab. It is found that for a stretching sheet ($\lambda > 0$) the

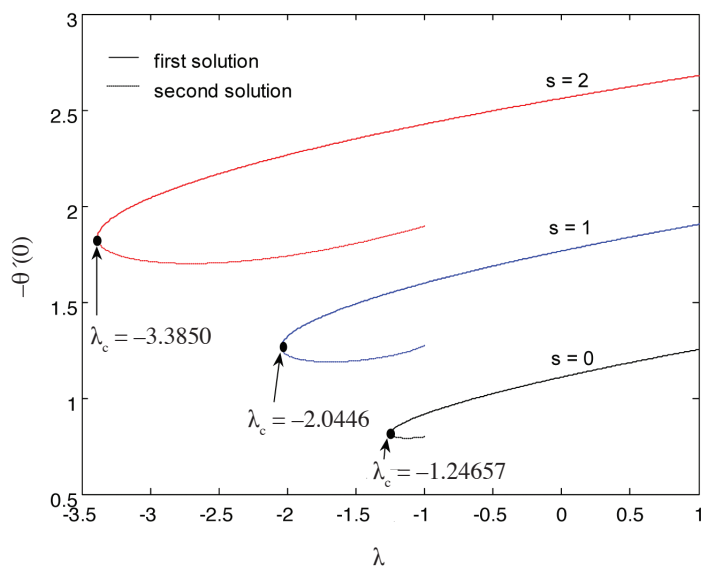


FIGURE 6. Variation of $-\theta'(0)$ with λ for $s = 0, 1, 2$ when $\phi = 0.1, Sc = 1$ and $\beta = 1$

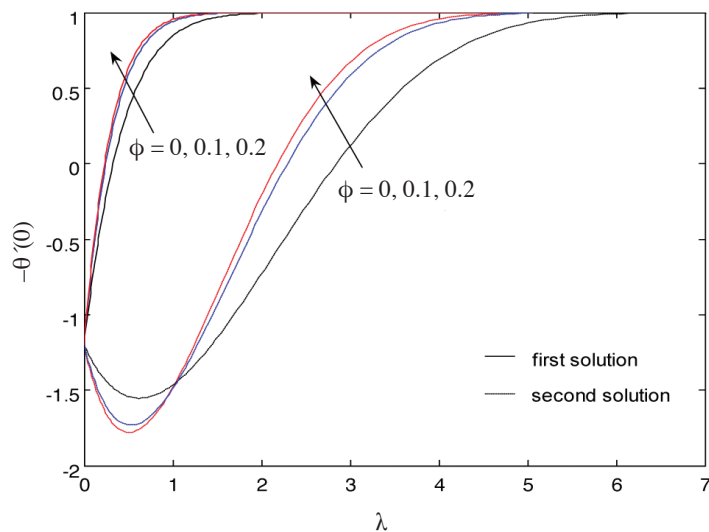


FIGURE 7. Velocity profiles $f'(\eta)$ for $\phi = 0, 0.1, 0.2$ when $s = 2, \lambda = -1.2, Sc = 1$ and $\beta = 1$

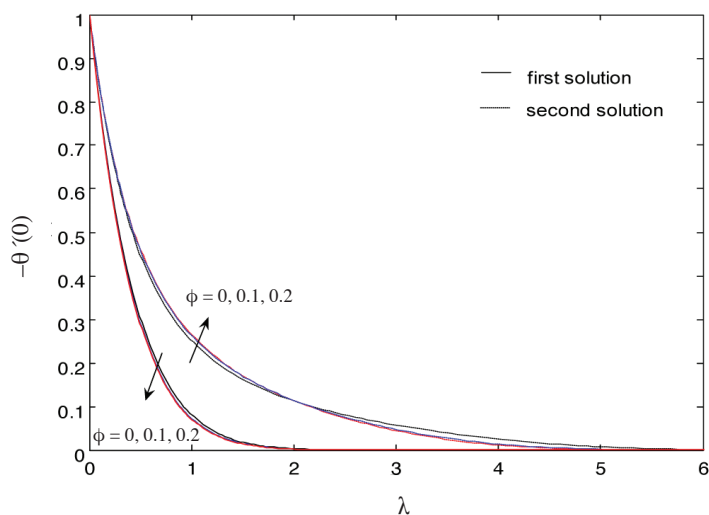


FIGURE 8. Concentration profiles $\theta(\eta)$ for $\phi = 0, 0.1, 0.2$ when $s = 2, \lambda = -1.2, Sc = 1$ and $\beta = 1$

TABLE 3. Values of the reduced skin friction $f''(0)$ and Sherwood number $-\theta'(0)$ for several values of λ , s and ϕ when $Sc = 1$ and $\beta = 1$

λ	s	ϕ	$f''(0)$	$-\theta'(0)$	λ	s	ϕ	$f''(0)$	$-\theta'(0)$
0	0	0.0	1.23259	1.09922	1	0	0.0	0	1.25331
		0.1	1.44798	1.10934			0.1	0	1.25331
		0.2	1.50135	1.11165			0.2	0	1.25331
	1	0.0	1.88931	1.75107		1	0.0	0	1.90427
		0.1	2.37112	1.76656			0.1	0	1.90427
		0.2	2.49823	1.77011			0.2	0	1.90427
	2	0.0	2.67006	2.54420		2	0.0	0	2.67942
		0.1	3.48040	2.56086			0.1	0	2.67942
		0.2	3.69849	2.56464			0.2	0	2.67942
0.1	0	0.0	1.14656	1.11594	10	0	0.0	-30.65468	2.16084
		0.1	1.34692	1.12507			0.1	-36.01146	2.08930
		0.2	1.39656	1.12716			0.2	-37.33874	2.07278
	1	0.0	1.73237	1.76759		1	0.0	-35.57635	2.81065
		0.1	2.17039	1.78136			0.1	-42.87969	2.73075
		0.2	2.28573	1.78452			0.2	-44.74278	2.71211
	2	0.0	2.42942	2.55851		2	0.0	-41.11677	3.53285
		0.1	3.16129	2.57332			0.1	-50.73593	3.44883
		0.2	3.35814	2.57669			0.2	-53.24375	3.42917

reduced skin friction increases as both s and ϕ increase, while dual solutions are found to exist for a shrinking sheet ($\lambda < 0$). Boundary layer thickness (both momentum and concentration) is higher for the second solution than for the first solution. In fact, the present paper extends that of Bhattacharyya (2011) to a nanofluid case.

ACKNOWLEDGEMENTS

This work was supported by a grant of the Romanian National Authority for Scientific Research, CNCS – UEFISCDI, project number PN-II-RU-TE-2011-3-0013. We also wish to express our thanks to the reviewer for the valuable comments and suggestions.

REFERENCES

- Bachok, N., Ishak, A. & Pop, I. 2010a. Boundary-layer flow of nanofluids over a moving surface in a flowing fluid. *International Journal of Thermal Sciences* 49: 1663-1668.
- Bachok, N., Ishak, A., Nazar R. & Pop I. 2010b. Flow and heat transfer at a general three-dimensional stagnation point in a nanofluid. *Physica B* 405: 4914-4918.
- Bhattacharyya, K. 2011. Dual solutions in boundary layer stagnation-point flow and mass transfer with chemical reaction past a stretching/shrinking sheet. *Int. Comm. Heat Mass Transfer* 38: 917-922.
- Brinkman, H.C. 1952. The viscosity of concentrated suspensions and solutions. *Journal of Chemical Physics* 20: 571-581.
- Buongiorno, J. 2006. Convective transport in nanofluids, *ASME J. Heat Transfer* 128: 240-250.
- Choi, S.U.S. 1995. Enhancing thermal conductivity of fluids with nanoparticles. *ASME Fluids Engng. Division* 231: 99-105.
- Crane, L.J. 1970. Flow past a stretching plate. *J. Appl. Math. Phys. (ZAMP)* 21: 645-647.
- Das, S.K., Choi, S.U.S., Yu, W. & Pradet, T. 2007. *Nanofluids: Science and Technology*. New Jersey: Wiley pp. 20.
- Ding, Y., Chen, H. Wang, L., Yang, C.-Y., He, Y., Yang, W., Lee, W.P., Zhang, L. & Huo, R. 2007. Heat transfer intensification using nanofluids. *KONA* 25: 23-38.
- Eagen, J., Rusconi, R., Piazza, R. & Yip, S. 2010. The classical nature of thermal conduction in nanofluids. *ASME J. Heat Transfer* 132: 102402.
- Fan, J. & Wang, L. 2011. Review of heat conduction in nanofluids. *ASME J. Heat Transfer* 133: 040801.
- Fang, T. 2008. Boundary layer flow over a shrinking sheet with power law velocity. *Int. J. Heat Mass Trans.* 51: 5838-5843.
- Fang, T., Liang, W. & Lee, C.F. 2008. A new solution branch for the Blasius equation—a shrinking sheet problem. *Comput. Math. Appl.* 56: 3088-3095.
- Fang, T., Zhang, J. & Yao, S. 2009. Viscous flow over an unsteady shrinking sheet with mass transfer. *Chin. Phys. Lett.* 26: 014703.
- Goldstein, S. 1965. On backward boundary layers and flow in converging passages. *J. Fluid Mech.* 21: 33-45.
- Gupta, P.S. & Gupta, A.S. 1977. Heat and mass transfer on a stretching sheet with suction and blowing. *Can. J. Chem. Eng.* 55: 744-746.
- Ishak, A., Lok, Y.Y. & Pop, I. 2010. Stagnation-point flow over a shrinking sheet in a micropolar fluid. *Chem. Eng. Commun.* 197: 1417-1427.
- Kakaç, S. & Pramuanjaroenkij, A. 2009. Review of convective heat transfer enhancement with nanofluids, *Int. J. Heat Mass Transfer* 52: 3187-3196.
- Khan, W.A. & Pop, I. 2010. Boundary-layer flow of a nanofluid past a stretching sheet, *Int. J. Heat Mass Transfer* 53: 2477-2483.
- Lee, J.H., Lee, S.H., Choi, C.J., Jang, S.P. & Choi, S.U.S. 2010. A review of thermal conductivity data, mechanics and models for nanofluids. *Int. J. Micro-Nano Scale Transport* 1: 269-322.

- Miklavčič, M. & Wang, C.Y. 2006. Viscous flow due a shrinking sheet. *Q. Appl. Math.* 64: 283-290.
- Oztop, H.F. & Abu-Nada, E. 2008. Numerical study of natural convection in partially heated rectangular enclosures filled with nanofluids. *International Journal of Heat and Fluid Flow* 29: 1326-1336.
- Shampine, L.F., Reichelt, M.W. & Kierzenka, J. 2010. Solving boundary value problems for ordinary differential equations in Matlab with bvp4c (http://www.mathworks.com/bvp_tutorial).
- Sparrow, E.M. & Abraham, J.P. 2005. Universal solutions for the streamwise variation of the temperature of a moving sheet in the presence of a moving fluid. *Int. J. Heat Mass Transfer* 48: 3047-3056.
- Tiwari, R.K. & Das, M.K. 2007. Heat transfer augmentation in a two-sided lid-driven differentially heated square cavity utilizing nanofluids. *International Journal of Heat and Mass Transfer* 50: 2002-2018.
- Wang, C.Y. 2008. Stagnation flow towards a shrinking sheet. *Int. J. Nonlinear Mech.* 43: 377-382.
- Wang, X.-Q. & Mujumdar, A.S. 2008. A review on nanofluids-part I: Theoretical and numerical investigations. *Brazilian Journal of Chemical Engineering* 25: 613-630.
- Wong, K.F.V. & Leon, O.D. 2010. Applications of nanofluids: current and future, *Adv. Mech. Eng.* 2010: 519659 11p.
- Yacob, N.A. Ishak, A. & Pop, I. 2011. Falkner-Skan problem for a static or moving wedge in nanofluids, *Int. J. Thermal Sci.* 50: 133-139.

Faculty of Mathematics and Computer Science
Babes-Bolyai University
400084 Cluj-Napoca, Romania

*Corresponding author; email: popm.ioan@yahoo.co.uk

Received: 19 April 2012

Accepted: 15 May 2012